Distributed Model Predictive Control of Switched Nonlinear Systems with Scheduled Mode Transitions

Mohsen Heidarinejad
Dept. of Electrical Engineering, University of California, Los Angeles, CA 90095

Jinfeng Liu
Dept. of Chemical & Materials Engineering, University of Alberta, Edmonton AB T6G 2V4, Canada

Panagiotis D. Christofides
Dept. of Chemical and Biomolecular Engineering, University of California, Los Angeles, CA 90095

Dept. of Electrical Engineering, University of California, Los Angeles, CA 90095

DOI 10.1002/aic.14003
Published online January 25, 2013 in Wiley Online Library (wileyonlinelibrary.com)

A method for the design of distributed model predictive control (DMPC) systems for a class of switched nonlinear systems for which the mode transitions take place according to a prescribed switching schedule is presented. Under appropriate stabilizability assumptions on the existence of a set of feedback controllers that can stabilize the closed-loop switched, nonlinear system, a cooperative DMPC architecture using Lyapunov-based model predictive control (MPC) in which the distributed controllers carry out their calculations in parallel and communicate in an iterative fashion to compute their control actions is designed. The proposed DMPC design is applied to a nonlinear chemical process network with scheduled mode transitions and its performance and computational efficiency properties in comparison to a centralized MPC architecture are evaluated through simulations. © 2013 American Institute of Chemical Engineers *AIChE J*, 59: 860–871, 2013

Keywords: process control, optimization, model predictive control, distributed control, chemical processes

Introduction

Due to changes in raw materials (feedstock), energy sources, product specifications, and market demands, control of switched nonlinear systems with scheduled mode transitions has received considerable attention in the context of chemical process control applications. From a stability analysis point of view, switched systems are well studied using multiple Lyapunov function[1] (MLF) and dwell-time[2] concepts (see also Refs. 3, 4 for results and references in this area). From a controller design standpoint, to achieve closed-loop stability, mode transition situations should be carefully accounted for in the control problem formulation and solution. In this direction, control of switched systems has been addressed using approaches based on Lyapunov functions, for example, Refs. 5–9 as well as optimal control theory, for example, Refs. 1, 10, 11. Furthermore, to achieve scheduled mode transitions in an optimal setting and accommodate input and state constraints, model predictive control (MPC) framework can be used to design control systems that can achieve these objectives. MPC is an online optimization-based approach, which takes advantage of a system model to compute a future manipulated input trajectory by minimizing a typically quadratic cost function involving penalties on the system state and control action (see, e.g., Ref. 12 for a comprehensive review of results on MPC).

Typically, MPC, including MPC of switched/hybrid systems, is studied within a centralized control framework in which all the manipulated inputs are calculated in a single MPC problem (see, e.g., Refs. 13–16 for results on MPC of hybrid systems). Because in the evaluation of the control actions by MPC online optimization problems need to be solved, the evaluation time of the MPC is a very important concern. Specifically, the MPC evaluation time strongly depends on the number of manipulated inputs as well as the dimensionality of the process model. As the number of manipulated inputs increases, as it is the case in the context of large-scale chemical plants, the evaluation time of centralized MPC may increase significantly. This may impede the ability of centralized MPC to carry out real-time calculations within the limits imposed by process dynamics and operating conditions. These control action evaluation problems may become more acute when additional constraints are imposed on the MPC as it is the case in the context of switched systems to properly force the closed-loop system state to follow a trajectory that meets the desired switching (operating) process schedule.

Distributed MPC (DMPC) is a feasible alternative to overcome the increasing computational complexity of centralized MPC; the reader may refer to Refs. 17–20 for results on

Correspondence concerning this article should be addressed to P. D. Christofides at pdc@seas.ucla.edu.

© 2013 American Institute of Chemical Engineers

DMPC of linear and nonlinear systems. DMPC takes advantage of cooperation and communication of the distributed predictive controllers, which communicate over a shared network, to reduce the computational burden of the corresponding centralized MPC solution at the cost of slight degradation of the closed-loop performance. Pertaining to the DMPC approach adopted in this work are the cooperative DMPC schemes, where each distributed controller optimizes the control actions for its actuators by minimizing a "global" cost accounting for the entire plant state and set of inputs.[18,20] However, at this point, there is no work on the DMPC of switched or hybrid systems.

Motivated by the lack of methodologies on the DMPC of nonlinear systems with prescribed switching schedule mode transitions, in this work, we present a framework for the design of DMPC systems for a broad class of switched nonlinear systems for which the mode transitions take place according to a prescribed switching schedule. Under appropriate stabilizability assumptions on the existence of a set of feedback controllers that can stabilize the closed-loop switched, nonlinear system, we design a Lyapunov-based iterative DMPC scheme with appropriate stability constraints that achieves stability of the switched closed-loop system and tracking of the prescribed switching policy. In terms of DMPC feasibility, the stability constraints make sure that at the moment of mode switching, the closed-loop system state is at the stability region of the new mode while the value of the Lyapunov function of the new mode (at the moment of entering the new mode) is smaller compared to the value of this Lyapunov function at the last time that the closed-loop system had switched into that mode.

The rest of this article is organized as follows. Section Preliminaries provides preliminaries and assumptions. Section DMPC of Switched Nonlinear Systems describes the DMPC scheme for switched nonlinear systems, whereas Sections Stability Analysis and Distributed Optimization Considerations deal with closed-loop stability and convergence analysis, respectively. The proposed DMPC scheme is applied to a nonlinear chemical process network with scheduled mode transitions in Section Application to a Chemical Process Network and its performance and computational efficiency properties in comparison to centralized MPC are evaluated through simulations. Finally, Section Conclusions concludes the article.

Preliminaries

Notation

The notation $|\cdot|$ is used to denote the Euclidean norm of a vector, while we use $|\cdot|_Q$ to denote the square of a weighted Euclidean norm, that is, $|x|_Q = x^T Q x$ for all $x \in R^n$. A continuous function $\alpha : [0, a) \to [0, \bar{a})$ is said to belong to class $\mathcal{K}$ if it is strictly increasing and satisfies $\alpha(0) = 0$. The symbol Ω_r is used to denote the set $\Omega_r := \{x \in R^{n_x} : V(x) \le r\}$, where V is a continuous differentiable, positive definite scalar function, and the operator '/' denotes set subtraction, that is, $A/B := \{x \in R^{n_x} : x \in A, x \notin B\}$. The symbol diag($v$) denotes a matrix whose diagonal elements are the elements of vector v and all the other elements are zeros. T denotes matrix transpose operation. The symbols $t_{k_r^{\text{in}}}$ and $t_{k_r^{out}}$ denote the time when, for the rth time, the system of consideration has switched in and out of the kth mode, respectively, that is, $\sigma(t_{k_r^{\text{in}}}^+) = \sigma(t_{k_r^{out}}^-) = k$. Also, we define $\mathcal{T}_{k,\text{in}} = \{t_{k_1^{\text{in}}}, t_{k_2^{\text{in}}}, \cdots\}$ and $\mathcal{T}_{k,out} = \{t_{k_1^{out}}, t_{k_2^{out}}, \cdots\}$ as the set of switching times at which the kth mode is switched in and out, respectively.

Class of switched nonlinear systems

We consider switched nonlinear systems which are composed of p modes (i.e., finite-number of switching modes) and in each mode, there are m interconnected subsystems. Each of the subsystems in a mode can be described by the following state-space model:

$$\dot{x}_i(t) = f_{i_{\sigma(t)}}(x) + g_{si_{\sigma(t)}}(x) u_{i_{\sigma(t)}}(t) \tag{1}$$

where $i = 1, \ldots, m$, $x_i(t) \in R^{n_{x_i}}$ denotes the vector of state variables of subsystem i, $u_{i_{\sigma(t)}}(t) \in R^{m_{u_i}}$ $(i = 1, \ldots, m)$ is the set of control (manipulated) inputs affecting the ith subsystem in σ mode. $\sigma : [0, \infty) \to \mathcal{I}$ denotes the switching signal which is assumed to be a piecewise continuous from the right function of time, that is, $\sigma(t_k) = \lim_{t \to t_k^+} \sigma(t)$ for all k, implying that only a finite number of switches is allowed over any finite interval of time. The variable $x \in R^{n_x}$ denotes the state of the entire nonlinear system which is composed of the states of the m subsystems, that is $x = \left[x_1^T \cdots x_i^T \cdots x_m^T\right]^T \in R^{n_x}$. In the subsystem model of Eq. 1, it is assumed that subsystems are coupled through system state only. The dynamics of x can be described as follows:

$$\dot{x}(t) = f_{\sigma(t)}(x) + \sum_{i=1}^{m} g_{i_{\sigma(t)}}(x) u_{i_{\sigma(t)}}(t) \tag{2}$$

where the vector function $f_{\sigma(t)}(x)$ and the matrix function $g_{i_{\sigma(t)}}(x)$ are appropriate compositions of $f_{i_{\sigma(t)}}$ and $g_{si_{\sigma(t)}}$ which have dimension $(n_x \times 1)$ and $(n_x \times m_{u_i})$, respectively. The m sets of inputs are restricted to be in m nonempty convex sets $U_{i_{\sigma(t)}} \subseteq R^{m_{u_i}}$, $i = 1, \ldots, m$, which are defined as $U_{i_{\sigma(t)}} := \{u_{i_{\sigma(t)}} \in R^{m_{u_i}} : |u_{i_{\sigma(t)}}| \le u_{i_{\sigma(t)}}^{\max}\}$, where $u_{i_{\sigma(t)}}^{\max}$, $i = 1, \ldots, m$, are the magnitudes of the input constraints. We will design m controllers to compute the m sets of control inputs $u_{i_{\sigma(t)}}$, $i = 1, \ldots, m$, respectively. We will refer to the controller computing $u_{i_{\sigma(t)}}$ as controller i at mode $\sigma(t)$. We assume that the switching signal takes its values in a finite index set $\mathcal{I} = \{1, 2, \ldots, p\}$.

We assume that the vector function f_k, and the matrix functions g_{i_k}, $i = 1, \ldots, m$ $(k \in \mathcal{I})$ are locally Lipschitz vector and matrix functions, respectively, and that the origin is an equilibrium point of the unforced system (i.e., system of Eq. 2 with $u_{i_k}(t) = 0$, $i = 1, \ldots, m$, for all t, $k \in \mathcal{I}$) which implies that $f_k(0) = 0$, $\forall k \in \mathcal{I}$. We further assume that during the system operation at mode k for rth time, that is, $t_{k_r^{\text{in}}} \le t < t_{k_r^{out}}$, the system state measurements are available and sampled at synchronous time instants $t_q = t_{k_r^{\text{in}}} + q\Delta_{k_r}$, $q = 0, 1, 2, \ldots, N_{k_r}$ where Δ_{k_r} is the sampling time. Without loss of generality, we assume that N_{k_r} is a positive integer.

Stabilizability assumptions on nonlinear switched system

Consider the system of Eq. 2, for a fixed $\sigma(t) = k$ for some $k \in \mathcal{I}$. We assume that there exists a feedback controller $h_k(x) = \left[h_{1_k}^T(x) \cdots h_{m_k}^T(x)\right]^T$ with $u_{i_k} = h_{i_k}(x)$, $i = 1, \ldots, m$, which renders the origin of the closed-loop system at mode k asymptotically stable while satisfying the input constraints for all the states x inside a given stability region. Using converse Lyapunov theorems,[21,22] this assumption implies that there exist class $\mathcal{K}$ functions $\alpha_{l_k}(\cdot), l = 1, 2, 3, 4$ and a

continuously differentiable Lyapunov function $V_k(x)$ for the closed-loop system, that satisfy the following inequalities:

$$\begin{aligned}
&\alpha_{1_k}(|x|) \le V_k(x) \le \alpha_{2_k}(|x|)\\
&\frac{\partial V_k(x)}{\partial x}(f_k(x)+\sum_{i=1}^{m} g_{i_k}(x)h_{i_k}(x)) \le -\alpha_{3_k}(|x|)\\
&\left|\frac{\partial V_k(x)}{\partial x}\right| \le \alpha_{4_k}(|x|)\\
&h_{i_k}(x) \in U_{i_k}, i=1,\ldots,m
\end{aligned} \tag{3}$$

for all $x \in D_k \subseteq R^{n_x}$ where D_k is an open neighborhood of the origin. We denote the region $\Omega_{\tilde{\rho}_k} \subseteq D_k$ as the stability region of the closed-loop system at mode k under the controller $h_k(x)$. Using the smoothness assumed for the f_k and g_{i_k}, and taking into account that the manipulated inputs u_{i_k}, $i=1,\ldots,m$, are bounded, there exists a positive constant M_k such that

$$\left|f_k(x)+\sum_{i=1}^{m} g_{i_k}(x)u_{i_k}\right| \le M_k \tag{4}$$

for all $x \in \Omega_{\tilde{\rho}_k}$, $u_{i_k} \in U_{i_k}$, $i=1,\ldots,m$, and $k \in \mathcal{I}$. In addition, by the continuous differentiable property of the Lyapunov function $V_k(x)$ and the smoothness of f_k and g_{i_k}, there exist positive constants L_{x_k}, $L_{u_{i_k}}$, and C_{gi_k} such that

$$\begin{aligned}
&\left|\frac{\partial V_k}{\partial x}f_k(x)-\frac{\partial V_k}{\partial x}f_k(x')\right| \le L_{x_k}|x-x'|\\
&\left|\frac{\partial V_k}{\partial x}g_{i_k}(x)-\frac{\partial V_k}{\partial x}g_{i_k}(x')\right| \le L_{u_{i_k}}|x-x'|, i=1,\ldots,m\\
&\left|\frac{\partial V_k}{\partial x}g_{i_k}(x)\right| \le C_{gi_k}, i=1,\ldots,m
\end{aligned} \tag{5}$$

for all $x, x' \in \Omega_{\tilde{\rho}_k}$, $u_{i_k} \in U_{i_k}$, $i=1,\ldots,m$, and $k \in \mathcal{I}$.

Stability properties of $h_k(x)$

In this subsection, we address the stability properties of the controller $h_k(x)$. Proposition 1 addresses the closed-loop stability properties of the controller $h_k(x)$, whereas Proposition 2 provides sufficient conditions to force the closed-loop system state under implementation of the Lyapunov-based controller in a sample-and-hold fashion to enter the corresponding stability region of the subsequent mode once the system switches to that mode.

We define the following sampled trajectory when the controller $h_k(x)$ is applied in a sample-and-hold fashion at mode k for $t_{k_r^{in}} \le \tau < t_{k_r^{out}}$ as follows

$$\begin{aligned}
\dot{\hat{x}}(\tau)=&f_k(\hat{x}(\tau))+\sum_{i=1}^{m} g_{i_k}(\hat{x}(\tau))h_{i_k}(\hat{x}(t_l)),\\
&l=0,1,\ldots,N_{kr}-1, \hat{x}(t_0)=x(t_{k_r^{in}})
\end{aligned} \tag{6}$$

where $t_0=t_{k_r^{in}}$.

Proposition 1 below ensures that if the closed-loop system at mode k controlled by $h_k(x)$ implemented in a sample-and-hold fashion and with open-loop state estimation (initial state) starts in $\Omega_{\tilde{\rho}_k}$ and stays in mode k for all times, then it is ultimately bounded in $\Omega_{\rho_{\min_k}}$. It characterizes the closed-loop stability region corresponding to each mode.

Proposition 1. (c.f. Ref. 20). Consider the closed-loop system of Eq. 6 and assume it operates at mode k for all times. Let $\Delta_k, \epsilon_{s_k} > 0$ and $\tilde{\rho}_k > \rho_{s_k} > 0$ satisfy:

$$-\alpha_{3_k}(\alpha_{2_k}^{-1}(\rho_{s_k}))+L'_{x_k}M_k\Delta_k \le -\epsilon_{s_k}/\Delta_k. \tag{7}$$

Then, if $\hat{x}(t_0) \in \Omega_{\tilde{\rho}_k}$ and $\rho_{\min_k} < \tilde{\rho}_k$, where $\rho_{\min_k} = \max\{V_k(\hat{x}(t+\Delta_{k_r})) : V_k(\hat{x}(t)) \le \rho_{s_k}\}$, $\forall \Delta_{k_r} \in (0, \Delta_k]$ the following inequality holds: $V_k(\hat{x}(t)) \le V_k(\hat{x}(t_q)), \forall t \in [t_q, t_{q+1})$ $(q=0,1,\ldots)$ and $V_k(\hat{x}(t_q)) \le \max\{V_k(\hat{x}(t_0))-q\epsilon_{s_k}, \rho_{\min_k}\}$. Since $V_k(\cdot)$ is a continuous function, $V_k(\hat{x}) \le \rho_{\min_k}$ implies $|\hat{x}| \le d_k$, where d_k is a positive constant and therefore, $\limsup_{t\to\infty} |\hat{x}(t)| \le d_k$.

For each mode $k \in \mathcal{I}$, we assume there exist a set of initial conditions $\Omega_{\tilde{\rho}_k}$, which is estimated as the level set of the Lyapunov function at mode k ($V_k(\cdot)$) and a positive real number ρ_k^* such that under implementation of the Lyapunov-based controller $h_k(\cdot)$ in a sample-and-hold fashion, the state of Eq. 6 satisfies

$$\dot{V}_k(\hat{x}(\tau)) \le -\rho_k^* V_k(\hat{x}(\tau)),\ \hat{x}(\tau) \in \Omega_{\tilde{\rho}_k/\rho_{s_k}},\ t_{k_r^{in}} \le \tau < t_{k_r^{out}} \tag{8}$$

Proposition 2. Consider the closed-loop sampled trajectory $\hat{x}(t)$ defined in Eq. 6. Given that $t_{k_r^{in}} \le t < t_{k_r^{out}} = t_{f_w^{in}}$, and $\hat{x}(t_{k_r^{in}}) \in \Omega_{\tilde{\rho}_k}$, if there exist $\tilde{\rho}_k > 0$, $\rho_k^* > 0$, $N_{k_r} > 0$ and $\Delta_{k_r} > 0$ $\forall k \in \mathcal{I}$ such that

$$\alpha_{2_f}(\alpha_{1_k}^{-1}(\tilde{\rho}_k e^{-\rho_k^* N_{k_r}\Delta_{k_r}})) \le \tilde{\rho}_f, \tag{9}$$

then $\hat{x}(t_{f_w^{in}}) \in \Omega_{\tilde{\rho}_f}$.

Proof. It can be obtained from Eq. 8 that

$$V_k(\hat{x}(t_{k_r^{out}})) \le V_k(\hat{x}(t_{k_r^{in}}))e^{-\rho_k^* N_{k_r}\Delta_{k_r}} \tag{10}$$

Since $\hat{x}(t_{k_r^{in}}) \in \Omega_{\tilde{\rho}_k}$, we have

$$V_k(\hat{x}(t_{k_r^{out}})) \le \tilde{\rho}_k e^{-\rho_k^* N_{k_r}\Delta_{k_r}} \tag{11}$$

From Eq. 3, we can obtain $|\hat{x}(t_{k_r^{out}})| \le \alpha_{1_k}^{-1}(\tilde{\rho}_k e^{-\rho_k^* N_{k_r}\Delta_{k_r}})$. If Eq. 9 is satisfied, using Eq. 3 for the Lyapunov-based controller at mode f, it can be concluded that $[V_f(\hat{x}(t_{f_w^{in}})) \le \tilde{\rho}_f$ which implies that $\hat{x}(t_{f_w^{in}}) \in \Omega_{\tilde{\rho}_f}$. □

Assumption 1. Consider the closed-loop system state trajectory of Eq. 6 and assume that $\hat{x}(t_{k_r^{in}}) \in \Omega_{\tilde{\rho}_k}$ Suppose, after switching out from mode k for rth time, the system switches to mode f for wth time, i.e., $t_{k_r^{out}} = t_{f_w^{in}}$. We assume that there exists $\epsilon^* > 0$ such that the closed-loop system state of Eq. 6 satisfies the following MLF constraint

$$V_f(\hat{x}(t_{f_w^{in}})) \le \begin{cases} V_f(\hat{x}(t_{f_{w-1}^{in}}))-\epsilon^* & ,\ w>1,\ V_f(\hat{x}(t_{f_{w-1}^{in}})) > \rho_{\min_f} \\ \rho_{\min_f} & ,\ w>1,\ V_f(\hat{x}(t_{f_{w-1}^{in}})) \le \rho_{\min_f} \\ \tilde{\rho}_f & ,\ w=1 \end{cases} \tag{12}$$

where $\rho_{\min_f}$ is defined in Proposition 1, $V_f(\hat{x}(t_{f_{w-1}^{in}}))$ is the value of the Lyapunov function of mode f when the system switches into mode f for $(w-1)^{th}$ time and $V_f(\hat{x}(t_{f_w^{in}}))$ is the value of the Lyapunov function of mode f when the system switches into mode f for wth time.

Assumption 1 implies that there exists a Lyapunov-based controller corresponding to each switching mode that meets the prescribed switching policy and at each mode the value of the Lyapunov function of the corresponding mode decreases to a certain level to ensure that when the system switches out of this mode to enter the subsequent mode, the closed-loop system state enters the stability region of the corresponding switching mode and the Lyapunov-based controllers of all the modes satisfy the MLF constraint.[1]

Remark 1. It should be emphasized that the stability region $\Omega_{\tilde{\rho}_k}$ characterizes the set of initial conditions starting from where, the closed-loop system state enters the

corresponding stability region of the subsequent mode to proceed at the time of the switch. From a feasibility point of view, the Lyapunov-based controller satisfying Assumption 1 yields a feasible solution to the prescribed switching policy. It should be emphasized that the purpose of the MPC formulation in this article (centralized or distributed) is to take advantage of this feasible solution to improve closed-loop performance.

Centralized MPC of switched systems

In this section, we briefly review the formulation of the centralized MPC for switched systems proposed in Ref. 14. For initialization purposes, we assume that $x(t_{1_1^{\text{in}}}) \in \Omega_{\tilde{\rho}_1}$. We assume that the system upon exiting from the mode k for the rth time enters mode f for the wth time (i.e., $t_{f_w^{\text{in}}} = t_{k_r^{out}} < \infty$). Specifically, the centralized MPC at mode k is formulated as follows:

$$\min_{u_{1_k},\ldots,u_{m_k} \in S(\Delta_{k_r})} \int_0^{\tilde{T}} \left[|\tilde{x}(\tau)|_{Q_{c_k}} + \sum_{i=1}^{m} |u_{i_k}(\tau)|_{R_{ci_k}} \right] d\tau \tag{13a}$$

$$st\ \dot{\tilde{x}}(\tau) = f_k(\tilde{x}(\tau)) + \sum_{i=1}^{m} g_{i_k}(\tilde{x}(\tau)) u_{i_k} \tag{13b}$$

$$u_{i_k}(\tau) \in U_{i_k}, i=1,\ldots,m \tag{13c}$$

$$\tilde{x}(0) = x(t_q) \tag{13d}$$

$$\frac{\partial V_k(x(t_q))}{\partial x} g_{i_k}(x(t_q)) u_{i_k}(0) \le \frac{\partial V_k(x(t_q))}{\partial x} g_{i_k}(x(t_q)) \times h_{i_k}(x(t_q)), i=1,\ldots,m \tag{13e}$$

$$V_f(\tilde{x}(t_{f_w^{\text{in}}})) \le \begin{cases} V_f(x(t_{f_{w-1}^{\text{in}}})) - \epsilon^* & , \ w>1,\ V_f(x(t_{f_{w-1}^{\text{in}}})) > \rho_{\min_f} \\ \rho_{\min_f} & , \ w>1,\ V_f(x(t_{f_{w-1}^{\text{in}}})) \le \rho_{\min_f} \\ \tilde{\rho}_f & , \ w=1 \end{cases} \tag{13f}$$

where $\tilde{x}$ is the predicted state trajectory of the closed-loop system, $S(\Delta_{k_r})$ is the family of piecewise continuous functions over $[0, \tilde{T}]$, Q_{c_k} and R_{ci_k}, $i=1,\ldots,m$, are positive definite weight matrices and $\tilde{T}$ is the time interval corresponding to prediction horizon and

$$\tilde{T} = \begin{cases} t_{k_r^{out}} - t_q, & \text{if } t_{k_r^{out}} < \infty \\ T_{\text{design}}, & \text{if } t_{k_r^{out}} = \infty \end{cases} \tag{14}$$

where $0 < T_{\text{design}} < \infty$ is a design parameter. The transition constraint of Eq. 13f ensures that if this mode is switched out and then switched back in, then $V_k(x(t_{k_{r+1}^{\text{in}}})) < V_k(x(t_{k_r^{\text{in}}}))$. In general $V_k(x(t_{k_r^{\text{in}}})) < V_k(x(t_{k_{r-1}^{\text{in}}})) < \cdots < \tilde{\rho}_k$. In other words, this constraint enforces the MLF stability condition in the switched system.

Remark 2. It should be emphasized that the centralized MPC of Eq. 13 is not implemented in the context of conventional receding horizon scheme. Based on the prescribed switching schedule policy, at each time interval that the system is supposed to operate in a specific mode, it uses a prediction horizon from the current time until the time that the system is supposed to switched out from that mode. Furthermore, if the system is supposed to operate in a single mode for a specific time, it uses a fixed horizon T_{design} based on Eq. 14.

The manipulated inputs of the centralized control design of Eq. 13 at mode k are defined as follows:

$$u_{i_k}(t) = u_{i_k}^*(t-t_q|t_q), i=1,\ldots,m, \forall t \in [t_q, t_{q+1}) \tag{15}$$

A potential drawback of the centralized MPC framework is that its computational burden significantly increases as the number of manipulated inputs and constraints grow, motivating the development of DMPC algorithms for switched systems.

DMPC of Switched Nonlinear Systems

In this section, we propose an iterative Lyapunov-based DMPC scheme for switched nonlinear systems given a prescribed switching sequence. We assume that there exists a Lyapunov-based controller for each of the switched system modes which satisfies Eqs. 3 and 8. The controller design problem seeks to enforce appropriate Lyapunov-based stability constraint in the DMPC formulation to achieve practical stability in the closed-loop switched system. From a control design perspective, DMPC forces the system state to evolve at each switching mode such that at the time of switching into the next mode, the closed-loop system state is within the stability region of the new mode. One of the difficulties in the implementation of DMPC in switched systems is the enforcement of the MLF constraint (Eq. 13f) from a feasibility point of view; however, in this work, we take advantage of the specified properties of the Lyapunov-based controller (Eqs. 3 and 8) to provide a feasible solution to the optimization problem of the DMPC for switched systems. Specifically, the implementation strategy of DMPC of switched nonlinear systems can be described as follows:

1. At sampling time t_q all of the distributed controllers receive the state measurements $x(t_q)$ through sensors.
2. At each iteration $c < c_{\max}$.
   - 2.1. All of the distributed controllers exchange their latest optimal input trajectories.
   - 2.2. Each MPC evaluates its own future input trajectory based on $x(t_q)$ and the latest received input trajectories of all the other MPCs.
   - 2.3. Using the computed input trajectories of all DMPCs the constraint of Eq. 13f is checked. If this constraint is satisfied go to Step 2.5; otherwise, go to Step 2.4.
   - 2.4. Provide the DMPCs a new initial guess by slightly perturbing the latest feasible optimal solution (if $c=1$, this solution is $h(x(t_q))$; for $c>1$, it is the solution obtained at iteration $c-1$) and recalculate the input trajectories of the DMPCs. If the new input trajectories satisfy the constraint of Eq. 13f, go to Step 2.5; otherwise, recalculate the input trajectories of the DMPCs by slightly perturbing the latest initial guess and check if the constraint of Eq. 13f is satisfied. If a new DMPC solution that satisfies the constraint of Eq. 13f cannot be found after a set number of evaluations, if $c=1$, use $h(x(t_q))$ as a solution, else, keep the solution obtained at iteration $c-1$. Go to Step 2.5.
   - 2.5. Set $c \leftarrow c+1$ and return to Step 2.1.
3. After a number of iterations/evaluations that depend on the sampling time, pick the input trajectories which yield the minimum cost function and satisfy the constraint of Eq. 13f over the iterations.
4. Each MPC controller sends the first step input value of its optimal input trajectory to its actuators.

At each sampling time and at first iteration, the Lyapunov-based controller of the corresponding mode is a feasible solution for the optimization problem of each DMPC of

Eq. 16 and also for the centralized MPC problem of Eq. 13; this is consequence of Assumption 1 which imposes the existence of a feasible control input trajectory for the centralized control problem for the switched systems and also because $h(x(t_q))$ is a feasible solution for the DMPCs.

According to this implementation strategy, the DMPC formulation of MPC j at iteration c is as follows:

$$\min_{u_{j_k}\in S(\Delta_{k_r})} \int_0^{\tilde{T}} \left[|\tilde{x}^j(\tau)|_{Q_{c_k}} + \sum_{i=1}^{m} |u_{i_k}(\tau)|_{R_{ci_k}} \right] d\tau \tag{16a}$$

$$st\ \dot{\tilde{x}}^j(\tau) = f_k(\tilde{x}^j(\tau)) + \sum_{i=1}^{m} g_{i_k}(\tilde{x}^j(\tau))u_{i_k} \tag{16b}$$

$$u_{i_k}(\tau) = u_{i_k}^{*,c-1}(\tau|t_q), \quad i \neq j \tag{16c}$$

$$u_{j_k}(\tau) \in U_{j_k} \tag{16d}$$

$$\tilde{x}^j(0) = x(t_q) \tag{16e}$$

$$\frac{\partial V_k(x(t_q))}{\partial x} g_{j_k}(x(t_q))u_{j_k}(0) \leq \frac{\partial V_k(x(t_q))}{\partial x} g_{j_k}(x(t_q))h_{j_k}(x(t_q)) \tag{16f}$$

$$V_f(\tilde{x}^j(t_{f_w^{\text{in}}})) \leq \begin{cases} V_f(x(t_{f_{w-1}^{\text{in}}})) - \epsilon^* & ,\ w > 1,\ V_f(x(t_{f_w^{\text{in}}})) > \rho_{\min_f} \\ \rho_{\min_f} & ,\ w > 1,\ V_f(x(t_{f_w^{\text{in}}})) \leq \rho_{\min_f} \\ \tilde{\rho}_f & ,\ w = 1 \end{cases} \tag{16g}$$

where $u_{i_k}^{*,c-1}(\tau|t_q)$ are the optimal control input trajectories from MPC i ($i=1,\ldots,m$, $i \neq j$) and $\tilde{x}^j$ is the predicted system state trajectory while MPC j uses the optimal control input trajectories of the rest of the controllers from iteration $c-1$. The constraint of Eq. 16f enforces that the amount of reduction in the value of the Lyapunov function by applying the control inputs of the DMPCs is at least at the level achieved by the Lyapunov-based controller when it is applied in a sample-and-hold fashion. $S(\Delta_{k_r})$ is the family of piecewise continuous functions over $[0, \tilde{T}]$. $\tilde{T}$ is the time interval corresponding to the prediction horizon which is chosen according to Eq. 14. The transition constraint of Eq. 16g ensures that if the f mode is switched out and then switched back in for the wth time, then $V_f(x(t_{f_w^{\text{in}}})) < V_f(x(t_{f_{w-1}^{\text{in}}}))$. In other words, this constraint enforces the MLF stability constraint in the switched system. If previously, the closed-loop system state entered the final invariant set $\Omega_{\rho_{min_f}}$, it will stay there. If it is the first time that the system switched to mode f, the closed-loop system state is restricted to the set $\Omega_{\tilde{\rho}_f}$.

It should be emphasized that at the first iteration ($c=1$), $h(x(t_q))$ is a feasible solution to the DMPC and each MPC assumes that the rest of the MPCs apply the Lyapunov-based controller at the current mode. The manipulated inputs of the proposed control design of Eq. 16 at mode k are defined as follows:

$$u_{i_k}(t) = u_{i_k}^*(t - t_q|t_q), i = 1,\ldots,m, \forall t \in [t_q, t_{q+1}). \tag{17}$$

Remark 3. Referring to the implementation of the DMPC of Eq. 16 with the objective of ensuring that the computed optimal solution satisfies the transition constraint of the centralized MPC of Eq. 18 at each sampling time, we can take advantage of a sequential implementation strategy at the cost of increasing the computational time of the DMPC calculation because in this case the computational time at each sampling time will be the sum of the computational times of all DMPCs involved in the sequential implementation. In the sequential architecture, if we evaluate MPCs in an increasing order and pass optimal solutions to the adjacent controller, $(h_1(x(t_q)),\ldots,h_m(x(t_q)))$ is a feasible control input used for MPC 1, $(u_1^*(t_q), h_2(x(t_q)),\ldots,h_m(x(t_q)))$ is a feasible control input used for MPC 2, where $u_1^*(t_q)$ is the optimal manipulated input obtained by MPC 1 at sampling time t_q and so on.

Remark 4. In this work, we consider that the subsystems are fully coupled through the entire system state. In this case, it is necessary that each controller has access to the entire system state measurements. However, it is possible to only use some of the states in certain distributed controllers by explicitly taking into account the system topology and interactions between subsystems.

Stability Analysis

The following theorem characterizes the stability properties of the DMPC design of Eq. 16.

Theorem 1. Consider the system of Eq. 2 in closed-loop under the DMPC of Eqs. 16 and 17 and assume that there exists Lyapunov-based controllers $h_k(\cdot)$, $\forall k \in \mathcal{I}$ satisfying Eq. 3 and Assumption 1. Let $0 < T_{\text{design}} < \infty$ be a design parameter, $\tilde{T}$ satisfy Eq. 14 and $t_{k_r^{\text{in}}} \leq t < t_{k_r^{out}} = t_{f_w^{\text{in}}}$ for some f, $k \in \mathcal{I}$. Then, given a positive real number d^{max}, if there exist $\Delta_k, \epsilon_{s_k} > 0$, $\tilde{\rho}_k > \rho_{s_k} > 0$ and $\epsilon_{w_k} > 0$ ($\forall k \in \mathcal{I}$) such that Eqs. 7 and 9 are satisfied and $\Delta_{k_r} \in (0, \Delta^*]$ where $\Delta^* = \min_{k\in\mathcal{I}} \Delta_k$, then $x(t)$ is bounded and $\limsup_{t\to\infty} |x(t)| \leq d^{max}$.

Proof. First we prove that the optimization problem of Eq. 16 is feasible at all times and then we proceed with the closed-loop stability analysis. Since the Lyapunov-based controller through implementation in a sample-and-hold fashion satisfies the MLF constraint of Eq. 13f and at the end of each switching mode it constraints the system state to enter the stability region of the subsequent mode, it follows that at each iteration $h_{j_k}(\cdot)$ is a feasible solution for the optimization problem of Eq. 16.

Given the radius of the ball around the origin, $d^{\max}$, the values of $\rho_{\min_k}$ and Δ_k $\forall k \in \mathcal{K}$ are computed based on Propositions 1 and 2. Then, for the purpose of DMPC implementation, a value of $\Delta_{k_r} \in (0, \Delta^*]$ is chosen where $\Delta^* = \min_{k\in\mathcal{I}} \Delta_k$ and $t_{k_r^{out}} - t_{k_r^{\text{in}}} = l_{k_r}\Delta_{k_r}$ for some integer $l_{k_r} > 0$ (note that given any two positive real numbers $t_{k_r^{out}} - t_{k_r^{\text{in}}}$ and Δ^*, one can always find a positive real number $\Delta_{k_r} \leq \Delta^*$ such that $t_{k_r^{out}} - t_{k_r^{\text{in}}} = l_{k_r}\Delta_{k_r}$ for some integer $l_{k_r} > 0$).

Part 1: First, consider the case when the switching is infinite. Let t be such that $t_{k_r^{\text{in}}} \leq t < t_{k_r^{out}}$ and $t_{f_w^{\text{in}}} = t_{k_r^{out}} < \infty$. Consider the active mode k. If $V_k(x) > \rho_{\min_k}$, the continued feasibility of the constraint of Eq. 16f implies that $V_k(x(t_{k_r^{out}})) < V_k(x(t_{k_r^{\text{in}}}))$. The transition constraint of Eq. 16g ensures that if this mode is switched out and then switched back in, then $V_k(x(t_{k_{r+1}^{\text{in}}})) < V_k(x(t_{k_r^{\text{in}}}))$. In general $V_k(x(t_{k_r^{\text{in}}})) < V_k(x(t_{k_{r-1}^{\text{in}}})) < \cdots < \tilde{\rho}_k$. Under the feasibility of the constraints of Eqs. 16f and 16g for all future times, the value of $V_k(x)$ continues to decrease. If the mode of this Lyapunov function is not active, there exists at least some $z \in \mathcal{I}$ such that mode z is active and Lyapunov function V_z continues to decrease until the time that $V_z \leq \rho_{\min_z}$ (this happens because there is a finite number of modes, even if the number of switches may be infinite). From this point onwards, Proposition 1 ensures that V_z continues to be less

than or equal to $\rho_{\min_z}$. Due to continuity of Lyapunov functions, there exists $d^{\max}$ such that $\limsup_{t\to\infty}|x(t)| \le d^{\max}$.

Part 2: For the case of a finite switching sequence, consider a t such that $t_{k_r^{in}} \le t < t_{k_r^{out}} = \infty$. Following a similar argument, $V_k(x(t_{k_r^{in}})) < V_k(x(t_{k_{r-1}^{in}})) < \cdots < \tilde{\rho}_k$. At the time of the switch to mode k, therefore, $x(t_{k_r^{in}}) \in \Omega_{\tilde{\rho}_k}$. From this point onwards, the DMPC is applied without any switching constraint, i.e., the constraint of Eq. 16g is removed. Since the DMPC at mode k is stabilizing, it follows that $\limsup_{t\to\infty}|x(t)| \le d^{\max}$. This completes the proof of Theorem. □

Remark 5. The purpose of Theorem 1, is to clarify under appropriate assumptions which include (I) existence of Lyapunov-based controllers corresponding to each mode that can asymptotically stabilize the closed-loop system at that switching mode, (II) satisfaction of the prescribed switching schedule by the Lyapunov-based controllers, and (III) picking appropriate finite prediction horizon according to Eq. 14, that the closed-loop system state under the DMPC of Eq. 16 is bounded in a final invariant set.

Distributed Optimization Considerations

In this section, we address the question of convergence of the solution of the DMPC to the one of the centralized MPC. It should be emphasized that for general nonlinear systems it is not possible to prove convergence of the iterations of the DMPC to the optimal centralized MPC cost at each sampling time due to the way the Lyapunov-based constraint of the centralized MPC is broken down into constraints imposed on the individual MPCs. However, under appropriate assumptions which include linear model, quadratic Lyapunov functions corresponding to each mode and an appropriate update rule in the DMPC iterations, it can be shown that the MPC optimization problem is convex and under a sufficiently large number of iterations, the optimal value of the objective function under the DMPC converges to the optimal value of the corresponding centralized MPC at each sampling time.

Specifically, we consider a class of switched, linear time-invariant systems with a state-space description of the form at mode $k \in \mathcal{I}$:

$$\dot{x}(t) = A_k x(t) + \sum_{i=1}^{m} B_{i_k} u_{i_k}(t) \tag{18}$$

where A_k and B_{i_k} $(i=1,\ldots,m)$ are constant matrices with appropriate dimensions. We assume, in accordance with Assumption 1, that there exist a set of quadratic Lyapunov functions $V_k = x^T P_k x$, $\forall k \in \mathcal{I}$, where P_k, are positive definite matrices, and a set of explicit feedback controllers $u_{i_k} = K_{i_k} x$, where K_{i_k} is a constant coefficient matrix, meet the prescribed switching schedule defined in section Preliminaries. We also assume that the input used as the initial guess in the optimization problem of MPC at iteration $c+1$ is computed according to the following expression

$$u_{j_k}^{c}(\tau|t_k) = (1-\tilde{w}_{j_k}) u_{j_k}^{c-1}(\tau|t_k) + \tilde{w}_{j_k} u_{j_k}^{*,c}(\tau|t_k) \tag{19}$$

where $\sum_{j=1}^{m} \tilde{w}_{j_k} = 1$ with $0 < \tilde{w}_{j_k} < 1$, $u_{j_k}^{*,c}$ is the optimal solution of controller j $(j=1,\ldots,m)$ at iteration c and $u_{j_k}^{c-1}$ is the input trajectory assumed by the rest of controllers for controller j at iteration c and mode k.

Corollary 1. Consider the switched, linear system of Eq. 18, assume that the conditions of Assumption 1 hold with $V_k = x^T P_k x$ and $u_{i_k} = K_{i_k} x$ and let the input to the optimization problem of MPC i of Eq. 16 at mode k (using $V_k = x^T P_k x$, $h_{i_k} = K_{i_k} x$ where $i=1,\ldots,m$ and the linear model of Eq. 18) at iteration c be defined according to Eq. 16. Let also $x(t_q) \in \Omega_{\tilde{\rho}_k}$. Then, if the iteration number $c \to \infty$, the optimal cost of the distributed optimization problem of Eqs. 16–19, at sampling time t_q converges to the optimal cost of the corresponding centralized MPC. Furthermore, if the corresponding centralized MPC asymptotically stabilizes the origin of the closed-loop system, the DMPC of Eq. 16 also asymptotically stabilizes the origin of the closed-loop system and the closed-loop cost of the DMPC converges to the one given by the centralized control system.

Proof. We first prove that the optimization problems for both the centralized and the DMPC are convex. Specifically, the optimization problem for the centralized MPC of Eq. 13 with $V_k = x^T P_k x$ and $h_{i_k}(x) = K_{i_k} x$ at sampling time t_q takes the following form:

$$\min_{u_{1_k},\ldots,u_{m_k} \in S(\Delta_{k_r})} \int_0^{\tilde{T}} \left[|\tilde{x}(\tau)|_{Q_{c_k}} + \sum_{i=1}^{m} |u_{i_k}(\tau)|_{R_{c_{i_k}}} \right] d\tau \tag{20a}$$

$$st\ \dot{\tilde{x}}(\tau) = A_k \tilde{x}(\tau) + \sum_{i=1}^{m} B_{i_k} u_{i_k} \tag{20b}$$

$$u_{i_k}(\tau) \in U_{i_k}, i=1,\ldots,m \tag{20c}$$

$$\tilde{x}(0) = x(t_q) \tag{20d}$$

$$\frac{\partial V_k(x(t_q))}{\partial x} B_{i_k} u_{i_k}(0) \le \frac{\partial V_k(x(t_q))}{\partial x} B_i K_{i_k} x(t_q), i=1,\ldots,m \tag{20e}$$

$$V_f(\tilde{x}(t_{f_w^{in}})) \le \begin{cases} V_f(x(t_{f_{w-1}^{in}})) - \epsilon^* & ,\ w>1,\ V_f(x(t_{f_{w-1}^{in}})) > \rho_{\min_f} \\ \rho_{\min_f} & ,\ w>1,\ V_f(x(t_{f_{w-1}^{in}})) \le \rho_{\min_f} \\ \tilde{\rho}_f & ,\ w=1 \end{cases} \tag{20f}$$

Specifically, the constraint of Eq. 20e takes the following form:

$$\begin{aligned} &(u_{i_k}(0)^T B_{i_k}^T P_k x(t_q) + x(t_q)^T P_k B_{i_k} u_{i_k}(0)) \\ &\le ((K_{i_k} x(t_q))^T B_{i_k}^T P_k x(t_q) + x(t_q)^T P_k B_{i_k} K_{i_k} x(t_q)) \end{aligned} \tag{21}$$

which is linear in terms of u_{i_k} $(i=1,\ldots,m)$. If we take into account that the input trajectories are piecewise constant and that $\tilde{x}(\tau) = e^{A\tau}\tilde{x}(t_q) + \int_0^{\tau} e^{A(\tau-s)} \sum_{i=1}^{m} (B_{i_k} u_{i_k}(s)) ds$, for $\tau \in [0, \tilde{T}]$, and quadratic Lyapunov functions are used, it can be verified that all the constraints are convex in terms of the control inputs. Since U_{i_k} is also convex for $i=1,\ldots,m$, it can be concluded that the switched centralized MPC optimization problem of Eq. 20 is convex. Since the centralized MPC optimization problem for switched linear systems is convex and it has been initialized by a feasible solution $h_{i_k}(x(t_q)) = K_{i_k} x(t_q)$ under Assumption 1 and the fact that $x(t_q) \in \Omega_{\tilde{\rho}_k}$, it has a unique optimal solution $u_k^* = (u_{1_k}^*, \ldots, u_{m_k}^*)$ which yields $J(u_k^*)$ at sampling time t_q, where $J(\cdot)$ is the quadratic cost function of the optimization problem (see Eq. 20a). Following a similar argument, it can be proved that the DMPC optimization problem of MPC j $(j=1,\ldots,m)$ at mode k is also convex. Next, we prove that the optimal inputs and the cost of the DMPC converge to the ones of the centralized MPC at a fixed sampling time as $c \to \infty$. The proof follows similar arguments to the proofs presented in Refs. 23, 24.

Defining $u_k^c=(u_{1_k}^c,\ldots,u_{m_k}^c)$ and the cost function by $J(u_k^c)$ at iteration c and mode k, where the update rule is defined in Eq. 19 while considering the fact that

$$u_k^{c+1}=\tilde{w}_{1_k}(u_{1_k}^{*,c+1},u_{2_k}^c,\ldots,u_{m_k}^c)+\cdots+\tilde{w}_{m_k}(u_{1_k}^c,\ldots,u_{(m-1)_k}^c,u_{m_k}^{*,c+1}) \tag{22}$$

we can obtain

$$\begin{aligned}J(u_k^{c+1})&=J(\tilde{w}_{1_k}(u_{1_k}^{*,c+1},u_{2_k}^c,\ldots,u_{m_k}^c)+\cdots+\tilde{w}_{m_k}(u_{1_k}^c,\ldots,u_{(m-1)_k}^c,u_{m_k}^{*,c+1}))\\&<\tilde{w}_{1_k}J(u_{1_k}^{*,c+1},u_{2_k}^c,\ldots,u_{m_k}^c)+\cdots+\tilde{w}_{m_k}J(u_{1_k}^c,\ldots,u_{(m-1)_k}^c,u_{m_k}^{*,c+1})\\&\leq\tilde{w}_{1_k}J(u_{1_k}^c,u_{2_k}^c,\ldots,u_{m_k}^c)+\cdots+\tilde{w}_{m_k}J(u_{1_k}^c,\ldots,u_{(m-1)_k}^c,u_{m_k}^c)=J(u_k^c)\end{aligned} \tag{23}$$

where the first inequality is the result of strict convexity of the cost function $J(\cdot)$ and the second one arises from optimality of the control inputs $u_{i_k}^{*,c}$ at iteration c where $i=1,\ldots,m$. So, through iterations over a fixed sampling time, the value of the cost function decreases. Since the cost function is positive definite and strictly convex and it is bounded from above by the value achieved by the Lyapunov-based controller, we can conclude that the value of the cost function converges to some value $\bar{J}$ as $c\to\infty$. Since the cost function $J(\cdot)$ is strictly convex and the level sets of the cost function are compact, there is a limit point $\tilde{u}_k=(\tilde{u}_{1_k},\ldots,\tilde{u}_{m_k})$ where $\bar{J}=J(\tilde{u}_k)$. We choose an index set $Z\subset\{0,1,2,\ldots\}$ such that the sequence $\{u_k^z\}_{z\in Z}$ converges to $\tilde{u}_k$. Furthermore, all iterations u_k^z are in the intersection of $U_{1_k}\times U_{2_k}\times\ldots U_{m_k}$, where $\times$ denotes cartesian product, and the level set $J\leq J(u_k^0)$. Thus, $\lim_{z\in Z,z\to\infty}J(u_k^z)=\bar{J}$. Note that the optimal solution u_k^* of the centralized problem of Eq. 20 is also a feasible solution to the DMPC problem. Subsequently, we prove that if $c\to\infty$, then $\tilde{u}_k\to u_k^*$. Using contradiction, assume $\tilde{u}_k\neq u_k^*$. Since $J(\cdot)$ is a strict convex function we can write

$$\nabla J(\tilde{u}_k)^T(u_k^*-\tilde{u}_k)\leq J(u_k^*)-J(\tilde{u}_k)\equiv\Delta J(u_k)<0 \tag{24}$$

From Eq. 24 and using contradiction, if we define

$$\Delta\tilde{u}_i^{*^T}=(\mathbf{0},\ldots,\mathbf{0},(u_{i_k}^*-\tilde{u}_{i_k})^T,\mathbf{0}) \tag{25}$$

where $\mathbf{0}$ are vector columns of zeros with appropriate dimensions, it can be easily shown that the following equation is satisfied for at least one i where $i=1,\ldots,m$

$$\nabla J(\tilde{u}_k)^T\Delta\tilde{u}_i^*\leq\frac{\Delta J(u_k)}{m}<0 \tag{26}$$

Suppose it holds for $i=1$. Using Taylor's expansion around $\tilde{u}_k$ for $\epsilon_k\in(0,1)$, $\delta_k\in(0,\epsilon)$, $c\to\infty$ and taking advantage of Eq. 26, we can write

$$\begin{aligned}J(\tilde{u}_{1_k}+\epsilon_k(u_{1_k}^*-\tilde{u}_{1_k}),\tilde{u}_{2_k},\ldots,\tilde{u}_{m_k})&=J(\tilde{u}_k)+\epsilon_k\nabla J(\tilde{u}_k)^T\Delta\tilde{u}_1^*\\&+\frac{1}{2}\epsilon_k^2\Delta\tilde{u}_1^{*^T}\nabla^2J(\tilde{u}_{1_k}+\epsilon_k(u_{1_k}^*-\tilde{u}_{1_k}),\tilde{u}_{2_k},\ldots,\tilde{u}_{m_k})\Delta\tilde{u}_1^*\\&\leq J(\tilde{u}_k)+\frac{\epsilon_k}{m}\Delta J(u_k)+\varsigma_k\epsilon_k^2<J(\tilde{u}_k)\end{aligned} \tag{27}$$

if ϵ_k is small enough such that $\frac{\epsilon_k}{m}\Delta u_k+\varsigma_k\epsilon_k^2$ is negative (this is always possible since $\Delta J(u_k)<0$) and ς_k is independent of c and ϵ_k. Since the iterative algorithms converges to $J(\tilde{u}_k)$ we can write

$$J(\tilde{u}_k)=\lim_{c\to\infty}J(u_{1_k}^{*,c},u_{2_k}^c,\ldots,u_{m_k}^c) \tag{28}$$

Also, from optimality of $u_{1_k}^{*,c}$, if $c\to\infty$, we can obtain

$$\lim_{c\to\infty}J(u_{1_k}^{*,c},u_{2_k}^c,\ldots,u_{m_k}^c)\leq J(\tilde{u}_{1_k}+\epsilon_k(u_{1_k}^*-\tilde{u}_{1_k}),\tilde{u}_{2_k},\ldots,\tilde{u}_{m_k}) \tag{29}$$

It should be emphasized that for $c\to\infty$, $u_{i_k}^c\to\tilde{u}_{i_k}$ where $i=1,\ldots,m$. Considering Eqs. 27–29, we can obtain

$$\begin{aligned}J(\tilde{u}_k)&=\lim_{c\to\infty}J(u_{1_k}^{*,c},u_{2_k}^c,\ldots,u_{m_k}^c)\\&\leq J(\tilde{u}_{1_k}+\epsilon_k(u_{1_k}^*-\tilde{u}_{1_k}),\tilde{u}_{2_k},\ldots,\tilde{u}_{m_k})<\tilde{J}(\tilde{u}_k)\end{aligned} \tag{30}$$

Therefore, $J(\tilde{u}_k)<J(\tilde{u}_k)$ which is a contradiction. Therefore, the assumption $\tilde{u}_k\neq u_k^*$ was not true. It can be concluded that $\tilde{u}_k=u_k^*$ when $c\to\infty$ and $J(\tilde{u}_k)=J(u_k^*)$. If $x(t_q)\in\Omega_{\tilde{\rho}_k}$ and the centralized MPC can asymptotically stabilize the origin of the closed-loop system, using the above arguments recursively for each sampling time, if $c\to\infty$ for each sampling time, it follows that the DMPC also asymptotically stabilizes the origin of the closed-loop system and the closed-loop cost converges to the one given by the centralized control system.

Remark 6. Note that a suitable partition of the control loops to the various distributed controllers may improve the possibility of convergence of the DMPC solution to the centralized MPC solution for the nonlinear case,[25] and further, it may be possible to derive convex approximations of the DMPC formulation for nonlinear systems for which it is possible to prove convergence of the DMPC solution to the centralized solution.

Application to a Chemical Process Network

The process considered in this study is a three vessel, reactor–separator system consisting of two continuously stirred tank reactors (CSTRs) and a flash tank separator shown in Figure 1.[26] The operation schedule requires switching between two available inlet streams consisting of pure reactant at different flow rates, concentrations, and temperatures. At mode $\sigma=\{1,2\}$ a feed stream to the first CSTR F_{10_σ} contains the reactant A which is converted into the desired product B. The effluent of the first CSTR along with additional fresh feed F_{20_σ} makes up the inlet to the second CSTR. The reactions $A\to B$ and $A\to C$ (referred to as 1 and 2, respectively) take place in the two CSTRs in series before the effluent from CSTR 2 is fed to a flash tank. The overhead vapor from the flash tank is condensed and recycled to the first CSTR, and the bottom product stream is removed. A

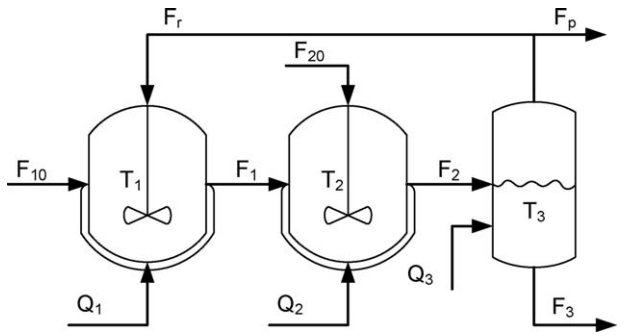

Figure 1. Two CSTRs and a flash tank with recycle stream.

small portion of the overhead is purged before being recycled to the first CSTR. All the three vessels are assumed to have static holdup. The dynamic equations describing the behavior of the system at mode σ, obtained through material and energy balances under standard modeling assumptions, are given below:

$$\frac{dT_1}{dt}=\frac{F_{10_\sigma}}{V_1}(T_{10_\sigma}-T_1)+\frac{F_r}{V_1}(T_3-T_1)+\frac{-\Delta H_1}{\rho C_p}k_1e^{\frac{-E_1}{RT_1}}C_{A1}+\frac{-\Delta H_2}{\rho C_p}k_2e^{\frac{-E_2}{RT_1}}C_{A1}+\frac{Q_{1_\sigma}}{\rho C_pV_1} \tag{31a}$$

$$\frac{dC_{A1}}{dt}=\frac{F_{10_\sigma}}{V_1}(C_{A10_\sigma}-C_{A1})+\frac{F_r}{V_1}(C_{Ar}-C_{A1})-k_1e^{\frac{-E_1}{RT_1}}C_{A1}-k_2e^{\frac{-E_2}{RT_1}}C_{A1} \tag{31b}$$

$$\frac{dC_{B1}}{dt}=\frac{-F_{10_\sigma}}{V_1}C_{B1}+\frac{F_r}{V_1}(C_{Br}-C_{B1})+k_1e^{\frac{-E_1}{RT_1}}C_{A1} \tag{31c}$$

$$\frac{dC_{C1}}{dt}=\frac{-F_{10_\sigma}}{V_1}C_{C1}+\frac{F_r}{V_1}(C_{Cr}-C_{C1})+k_2e^{\frac{-E_2}{RT_1}}C_{A1} \tag{31d}$$

$$\frac{dT_2}{dt}=\frac{F_1}{V_2}(T_1-T_2)+\frac{(F_{20_\sigma})}{V_2}(T_{20_\sigma}-T_2)+\frac{-\Delta H_1}{\rho C_p}k_1e^{\frac{-E_1}{RT_2}}C_{A2}+\frac{-\Delta H_2}{\rho C_p}k_2e^{\frac{-E_2}{RT_2}}C_{A2}+\frac{Q_{2_\sigma}}{\rho C_pV_2} \tag{31e}$$

$$\frac{dC_{A2}}{dt}=\frac{F_1}{V_2}(C_{A1}-C_{A2})+\frac{(F_{20_\sigma})}{V_2}(C_{A20_\sigma}-C_{A2})-k_1e^{\frac{-E_1}{RT_2}}C_{A2}-k_2e^{\frac{-E_2}{RT_2}}C_{A2} \tag{31f}$$

$$\frac{dC_{B2}}{dt}=\frac{F_1}{V_2}(C_{B1}-C_{B2})-\frac{(F_{20_\sigma})}{V_2}C_{B2}+k_1e^{\frac{-E_1}{RT_2}}C_{A2} \tag{31g}$$

$$\frac{dC_{C2}}{dt}=\frac{F_1}{V_2}(C_{C1}-C_{C2})-\frac{(F_{20_\sigma})}{V_2}C_{C2}+k_2e^{\frac{-E_2}{RT_2}}C_{A2} \tag{31h}$$

$$\frac{dT_3}{dt}=\frac{F_2}{V_3}(T_2-T_3)-\frac{H_{vap}F_r}{\rho C_pV_3}+\frac{Q_{3_\sigma}}{\rho C_pV_3} \tag{31i}$$

$$\frac{dC_{A3}}{dt}=\frac{F_2}{V_3}(C_{A2}-C_{A3})-\frac{F_r}{V_3}(C_{Ar}-C_{A3}) \tag{31j}$$

$$\frac{dC_{B3}}{dt}=\frac{F_2}{V_3}(C_{B2}-C_{B3})-\frac{F_r}{V_3}(C_{Br}-C_{B3}) \tag{31k}$$

$$\frac{dC_{C3}}{dt}=\frac{F_2}{V_3}(C_{C2}-C_{C3})-\frac{F_r}{V_3}(C_{Cr}-C_{C3}) \tag{31l}$$

Table 1. Process Variables

C_{A1}, C_{A2}, C_{A3}	Concentrations of A in vessels 1, 2, 3
C_{B1}, C_{B2}, C_{B3}	Concentrations of B in vessels 1, 2, 3
C_{C1}, C_{C2}, C_{C3}	Concentrations of C in vessels 1, 2, 3
C_{Ar}, C_{Br}, C_{Cr}	Concentrations of A, B, C in the recycle
T_1, T_2, T_3	Temperatures in vessels 1, 2, 3
T_{10_σ}, T_{20_σ}	Feed stream temperatures to vessels 1, 2 at mode $\sigma=\{1, 2\}$
F_1, F_2, F_3	Effluent flow rates from vessels 1, 2, 3
F_{10_σ}, F_{20_σ}	Feed stream flow rates to vessels 1, 2 at mode $\sigma=\{1, 2\}$
C_{A10_σ}, C_{A20_σ}	Concentrations of A in the feed stream to vessels 1, 2 at mode $\sigma=\{1, 2\}$
F_r	Recycle flow rate
V_1, V_2, V_3	Volumes of vessels 1, 2, 3
u_1, u_2, u_3	Manipulated inputs
E_1, E_2	Activation energy for reactions 1, 2
k_1, k_2	Preexponential values for reactions 1, 2
ΔH_1, ΔH_2	Heats of reaction for reactions 1, 2
H_{vap}	Heat of vaporization
α_A, α_B, α_C, α_D	Relative volatilities of A, B, C, D
MW_A, MW_B, MW_C	Molecular weights of A, B, C
Q_1, Q_2, Q_3	Heat inputs into vessels 1, 2, 3
C_p, R, ρ	Heat capacity, gas constant, and solution density

Each of the tanks has an external heat input/removal actuator. The model of the flash tank separator is derived under the assumption that the relative volatility for each of the species remains constant within the operating temperature range of the flash tank. This assumption allows calculating the mass fractions in the overhead based upon the mass fractions in the liquid portion of the vessel. It has also been assumed that there is a negligible amount of reaction taking place in the separator. The following algebraic equations model the composition of the overhead stream relative to the composition of the liquid holdup in the flash tank:

$$C_{Ar}=\frac{\alpha_AC_{A3}}{K},\quad C_{Br}=\frac{\alpha_BC_{B3}}{K},\quad C_{Cr}=\frac{\alpha_CC_{C3}}{K}$$
$$K=\alpha_AC_{A3}\frac{MW_A}{\rho}+\alpha_BC_{B3}\frac{MW_B}{\rho}+\alpha_CC_{C3}\frac{MW_C}{\rho}+\alpha_Dx_D\rho \tag{32}$$

where x_D is the mass fraction of the solvent in the flash tank liquid holdup and is found from a mass balance. The definitions for the variables used in Eqs. 31 and 32 can be found in Table 1, with the parameter values given in Table 2.

Table 2. Parameter Values

$T_{10_1}=300$, $T_{20_1}=300$	K
$T_{10_2}=301$, $T_{20_2}=327$	K
$F_{10_1}=5$, $F_{20_1}=5$, $F_r=1.9$	$\frac{m^3}{h}$
$F_{10_2}=5$, $F_{20_2}=5$	$\frac{m^3}{h}$
$C_{A10_1}=4$, $C_{A20_1}=3$	$\frac{kmol}{m^3}$
$C_{A10_2}=4.69$, $C_{A20_2}=3.25$	$\frac{kmol}{m^3}$
$V_1=1.0$, $V_2=0.5$, $V_3=1.0$	m^3
$E_1=5E4$, $E_2=5.5E4$	$\frac{kJ}{kmol}$
$k_1=3E6$, $k_2=3E6$	$\frac{1}{h}$
$\Delta H_1=-5E4$, $\Delta H_2=-5.3E4$	$\frac{kJ}{kmol}$
$H_{vap}=5$	$\frac{kJ}{kmol}$
$C_p=0.231$	$\frac{kJ}{kgK}$
$R=8.314$	$\frac{kJ}{kmolK}$
$\rho=1000$	$\frac{kg}{m^3}$
$\alpha_A=2$, $\alpha_B=1$, $\alpha_C=1.5$, $\alpha_D=3$	Unitless
$MW_A=50$, $MW_B=50$, $MW_C=50$	$\frac{kJ}{kmol}$

This process is divided into three subsystems corresponding to the first CSTR, the second CSTR, and the separator, respectively. For the three subsystems, we will refer to them as subsystem 1, subsystem 2, and subsystem 3, respectively. The state of subsystem 1 is defined as the deviations of the temperature and species concentrations in the first CSTR from the desired, operating steady state; that is, $x_1^T=[T_1-T_{1s_\sigma}\ C_{A1}-C_{A1s_\sigma}\ C_{B1}-C_{B1s_\sigma}\ C_{C1}-C_{Cs_\sigma}]^T$ for the system at mode σ. Similarly, we define the state of subsystems 2 and 3. Accordingly, the state of the whole process is defined as a combination of the states of the three subsystems; that is, $x^T=[x_1^T\ x_2^T\ x_3^T]$.

The process has one unstable and two stable steady states. The control objective is to regulate the process at the unstable steady-state x_{s_2} corresponding to the operating point defined by $Q_{1s}=Q_{2s}=Q_{3s}=0\ \frac{kJ}{h}$ (which are the same for both process operating modes), respectively. The values of the operating steady states corresponding to each mode are shown in Tables 3 and 4. Each of the tanks has an external heat input which is the control input associated with each subsystem, that is, $u_{1_\sigma}=Q_1-Q_{1s}$, $u_{2_\sigma}=Q_2-Q_{2s}$, and $u_{3_\sigma}=Q_3-Q_{3s}$ for $\sigma=1,2$. For mode 1, the inputs are subject to constraints as follows: $|u_{1_1}|\le 1.5\times10^5\ kJ/h$, $|u_{2_1}|\le 1.5\times10^5\ kJ/h$, and $|u_{3_1}|\le 2\times10^5\ kJ/h$, whereas in mode 2 $|u_{1_2}|\le 10^5\ kJ/h$, $|u_{2_2}|\le 10^5\ kJ/h$, and $|u_{3_2}|\le 1.33\times10^5\ kJ/h$. Three DMPC controllers (controller 1, controller 2, and controller 3) will be designed to manipulate each one of the three inputs in the three subsystems, respectively. Furthermore, we assume that the system state, x, is available at synchronous time instants $t_q=q\Delta$, $q=0,1,\ldots$, with $\Delta=0.001$ $h=3.6$ s to all the controllers. The process model belongs to the following class of nonlinear systems:

$$\dot{x}(t)=f_\sigma(x(t))+\sum_{i=1}^{3} g_{i_\sigma}(x(t))u_{i_\sigma}(t)$$

where the explicit expressions of f_σ, g_{i_σ} ($i=1,2,3$ and $\sigma=\{1,2\}$), are omitted for brevity.

In the simulations, we consider a quadratic Lyapunov function $V_\sigma(x)=x^TP_\sigma x$ with $P_1=diag([1010^3 10^3 10^3 2010^3\ 10^3 10^3 1010^3 10^3 10^3])$ and $P_2=diag([1010^3 10^3 10^3 1010^3 10^3\ 10^3 1010^3 10^3 10^3])$. We design the Lyapunov-based controller $h_\sigma(x)$ following the continuous bounded control law design[21,27] as follows:

$$u_\sigma=[u_{1_\sigma}u_{3_\sigma}u_{3_\sigma}]^T=h_\sigma(x)=-p_\sigma(x)(L_{G_\sigma}V_\sigma)^T \qquad (33)$$

Table 3. Steady-State Values for x_{s_1}

C_{A1s_1}	**3.31** $\left[\frac{kmol}{m^3}\right]$	C_{A2s_1}	**2.75** $\left[\frac{kmol}{m^3}\right]$	C_{A3s_1}	**2.88** $\left[\frac{kmol}{m^3}\right]$
C_{B1s_1}	0.17 $\left[\frac{kmol}{m^3}\right]$	C_{B2s_1}	0.45 $\left[\frac{kmol}{m^3}\right]$	C_{B3s_1}	0.50 $\left[\frac{kmol}{m^3}\right]$
C_{C1s_1}	0.04 $\left[\frac{kmol}{m^3}\right]$	C_{C2s_1}	0.11 $\left[\frac{kmol}{m^3}\right]$	C_{C3s_1}	0.12 $\left[\frac{kmol}{m^3}\right]$
T_{1s_1}	369.53 [K]	T_{2s_1}	435.25 [K]	T_{3s_1}	435.25 [K]

Table 4. Steady-State Values for x_{s_2}

C_{A1s_2}	3.32 $\left[\frac{kmol}{m^3}\right]$	C_{A2s_2}	2.69 $\left[\frac{kmol}{m^3}\right]$	C_{A3s_2}	2.91 $\left[\frac{kmol}{m^3}\right]$
C_{B1s_2}	0.34 $\left[\frac{kmol}{m^3}\right]$	C_{B2s_2}	0.70 $\left[\frac{kmol}{m^3}\right]$	C_{B3s_2}	0.85 $\left[\frac{kmol}{m^3}\right]$
C_{C1s_2}	0.08 $\left[\frac{kmol}{m^3}\right]$	C_{C2s_2}	0.17 $\left[\frac{kmol}{m^3}\right]$	C_{C3s_2}	0.20 $\left[\frac{kmol}{m^3}\right]$
T_{1s_2}	370.98 [K]	T_{2s_2}	429.65 [K]	T_{3s_2}	429.64 [K]

where

$$p_\sigma(x)=\begin{cases}\dfrac{L_{f_\sigma}V_\sigma+\sqrt{(L_{f_\sigma}V_\sigma)^2+(u^{\max}|L_{G_\sigma}V_\sigma^T|)^4}}{|L_{G_\sigma}V_\sigma^T|^2\left[1+\sqrt{1+(u^{max}|L_{G_\sigma}V_\sigma^T|)^2}\right]}, & L_{G_\sigma}V_\sigma\neq 0\\ 0, & L_{G_\sigma}V_\sigma=0\end{cases}$$

with $L_{f_\sigma}V_\sigma=\frac{\partial V_\sigma}{\partial x}f_\sigma(x)$ and $L_{G_\sigma}V_\sigma=\frac{\partial V_\sigma}{\partial x}G_\sigma(x)$, where $G_\sigma=[g_{1_\sigma}g_{2_\sigma}g_{3_\sigma}]$ being the Lie derivatives of the scalar function V_σ with respect to f_σ and G_σ, respectively. Note that $G_1=G_2$ in this example. To estimate the stability region $\Omega_{\tilde{\rho}_\sigma}$, extensive simulations were carried out to get an estimate of the region of the closed-loop system under Lyapunov-based control $h_\sigma(x)$ where the time-derivative of the Lyapunov function is negative, and then $\Omega_{\tilde{\rho}_\sigma}$ is defined as a level set of the Lyapunov function $V_\sigma(x)$ embedded within this region.

To carry out the closed-loop performance evaluation, we have computed the total cost of each simulation based on an index of the following form:

$$J=\sum_{i=0}^{M}\left[x(t_i)^TQ_{c_\sigma}x(t_i)+\sum_{j=1}^{3}u_{j_\sigma}(t_i)^TR_{cj_\sigma}u_{j_\sigma}(t_i)\right] \qquad (34)$$

where $t_0=0$ is the initial time of the simulations, $t_M=0.1$ h is the end time of the simulations, and $t_{i+1}=t_i+\Delta$ for $i=0,1,\ldots$. In the design of the controllers, the weighting

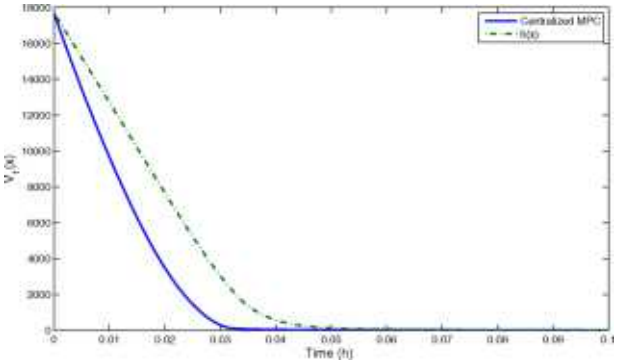

Figure 2. Lyapunov function trajectory of the closed-loop system under the implementation of the Lyapunov-based controller (dashed–dotted line) in a sample-and-hold fashion and of the centralized MPC (solid line) at mode one.

[Color figure can be viewed in the online issue, which is available at wileyonlinelibrary.com.]

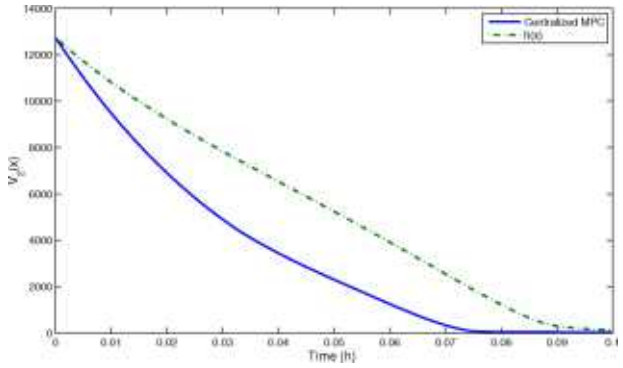

Figure 3. Lyapunov function trajectory of the closed-loop system under the implementation of the Lyapunov-based controller (dashed–dotted line) in a sample-and-hold fashion and of the centralized MPC (solid line) at mode two.

[Color figure can be viewed in the online issue, which is available at wileyonlinelibrary.com.]

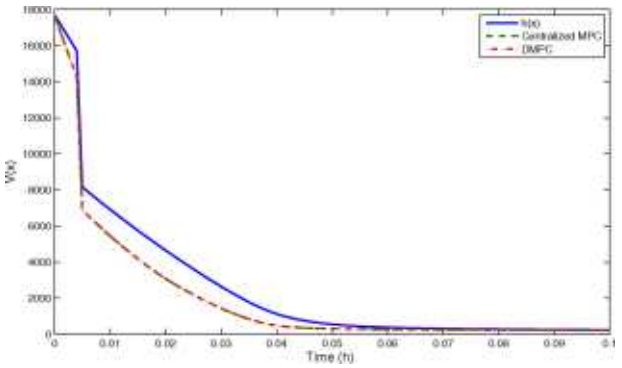

Figure 4. Lyapunov function trajectory of the closed-loop system under the implementation of the Lyapunov-based controller (solid line) in a sample-and-hold fashion, centralized MPC of Eq. 13 (*) and DMPC of Eq. 16 (dashed–dotted line) for the given switching policy; the line composed of the (*) and the dashed–dotted line overlap.

From $t=0$ to 0.004 h, the lines show $V_1(x)$ and from $t=0.004$ to 0.1 h, the lines show $V_2(x)$. [Color figure can be viewed in the online issue, which is available at wileyonlinelibrary.com.]

matrices are chosen to be $Q_{c_1}=Q_{c_2}=diag([1010^3 10^3 10^3 2010^3 10^3 10^3 1010^3 10^3 10^3])$ and $R_{1_1}=R_{2_1}=R_{3_1}=R_{1_2}=R_{2_2}=R_{3_2}=10^{-8}$. We set the number of iterations between controllers $c_{\max}=2$. The simulations were carried out using Java programming language in a Pentium 3.20 GHz computer. The optimization problems in MPC were solved using the open-source interior point optimizer Ipopt.

We first carried out simulations to illustrate that the Lyapunov-based controller and the centralized MPC scheme achieve practical closed-loop stability in each mode of operation, respectively. Figures 2 and 3 show the Lyapunov function trajectory in the closed-loop system under the Lyapunov-based controller implemented in a sample-and-hold fashion and the centralized MPC scheme at mode one and two, respectively. As it can be seen from these two figures, both control schemes at each mode achieve practical closed-loop stability, while the centralized MPC requests more aggressive moves to steer the closed-loop system state to the origin. From a closed-loop performance point of view, the centralized MPC outperforms the Lyapunov-based controller by 30% at mode one and 28% at mode two, respectively, in terms of the performance metric of Eq. 34.

As a scheduling policy, we assume that at time $t=0.004$ h, the process switches from mode 1 to mode 2. It should be emphasized that after the system enters mode 2, it stays there until the end of the simulation time ($t_f=0.1$ h), and the MPC/DMPC of mode 2 is used. Figure 4 compares the Lyapunov function trajectory of the closed-loop system under the Lyapunov-based controller implemented in a sample-and-hold fashion, the centralized MPC of Eq. 13 and the

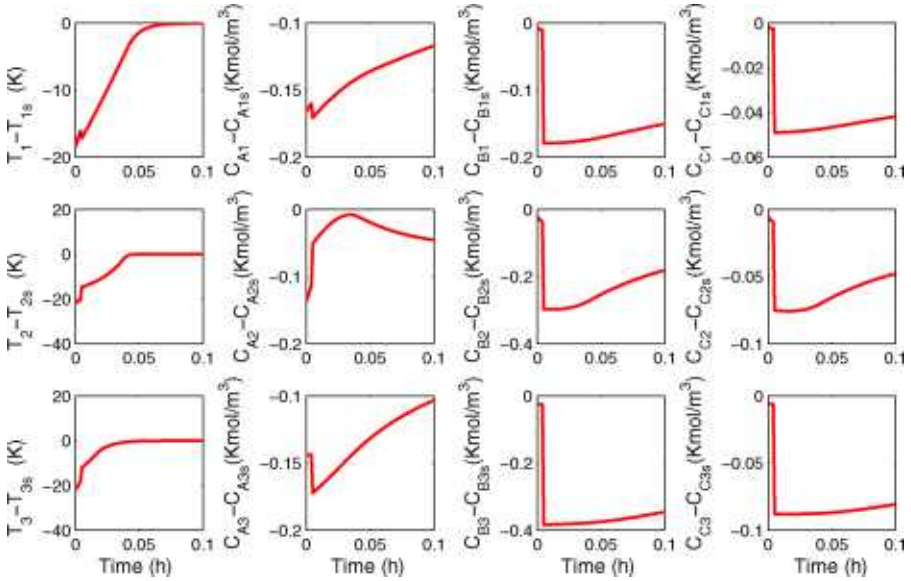

Figure 5. State trajectories of the closed-loop system under the implementation of the DMPC system of Eq. 16.

[Color figure can be viewed in the online issue, which is available at wileyonlinelibrary.com.]

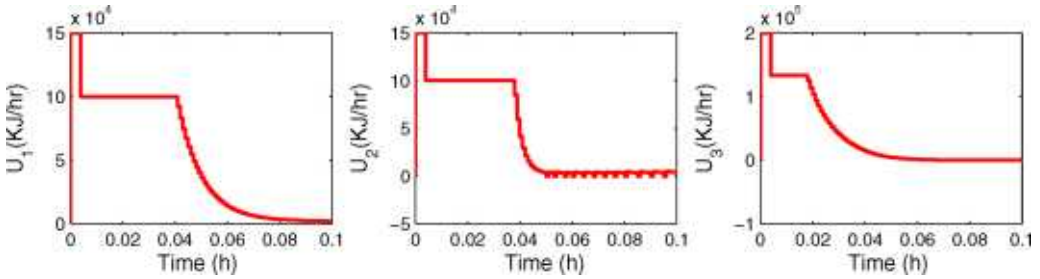

Figure 6. Manipulated input trajectories computed by the DMPC of Eq. 16.

[Color figure can be viewed in the online issue, which is available at wileyonlinelibrary.com.]

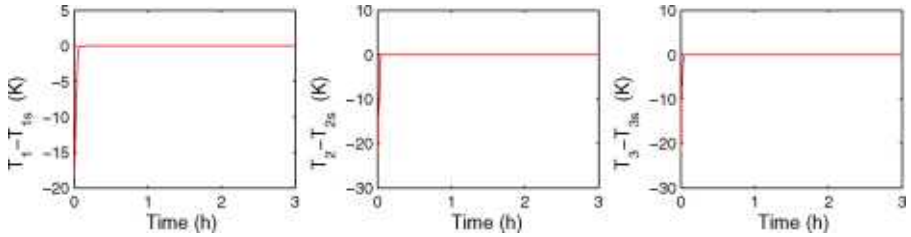

Figure 7. Temperature trajectories of the closed-loop system under the implementation of the DMPC system of Eq. 16.

[Color figure can be viewed in the online issue, which is available at wileyonlinelibrary.com.]

DMPC of Eq. 16 for a given switching policy, respectively. It illustrates that the Lyapunov-based controller can meet the given schedule by steering the closed-loop system state to the stability region of mode 2 at the time of the switch. So, for the given switching policy, the Lyapunov-based controller provides a feasible solution. Figure 4 shows the Lyapunov function trajectory of the closed-loop system under the implementation of the centralized MPC scheme subject to the switching constraint. As it can be seen from Figure 4, the MPC (both centralized and distributed) design enforces the appropriate constraint to steer the closed-loop system state at mode 1 to the stability region of mode 2 at the time of the switch. In Figure 4, the Lyapunov function is computed for each mode, independently. It should be emphasized that the MPC designs require more aggressive control actions to enter the stability region of mode 2 and subsequently stabilizing the plant compared to the Lyapunov-based controller, which yields improvement in terms of closed-loop performance.

Figures 5 and 6 depict the state and manipulated inputs in the closed-loop system under the DMPC design of Eq. 16 subject to the same switching schedule, respectively. Figure 5 shows the deviation of the state trajectories from their corresponding steady-state values at each mode. As it can be seen in these figures, the proposed DMPC design enforces the appropriate constraints to steer the closed-loop system state to the stability region of mode two at the time of the switch and subsequently, achieves practical closed-loop

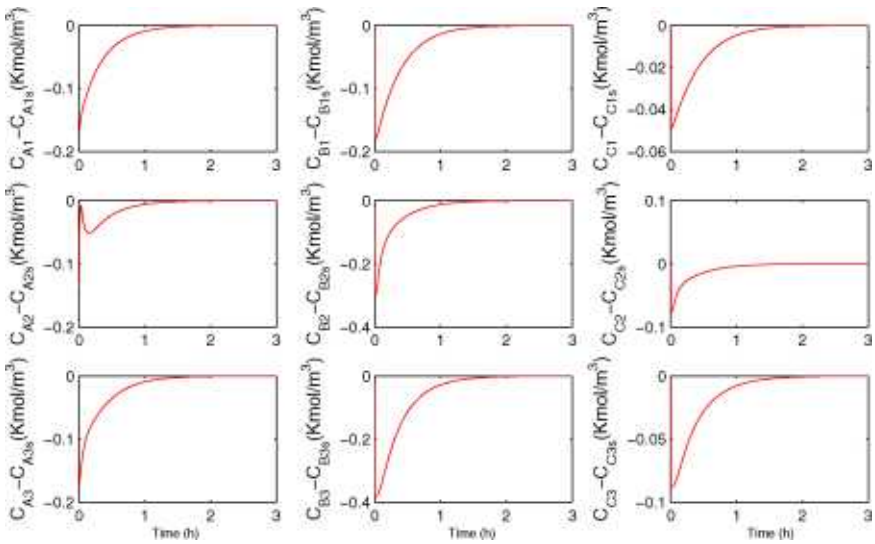

Figure 8. Concentration trajectories of the closed-loop system under the implementation of the DMPC system of Eq. 16.

[Color figure can be viewed in the online issue, which is available at wileyonlinelibrary.com.]

stability. Note that the DMPC is able to drive the states to their steady-state values as shown in Figures 7 and 8. From a closed-loop performance point of view based on Eq. 34, the centralized MPC formulation of Eq. 13 yields 236447.02 in cost function value J, whereas the DMPC design of Eq. 16 yields 236446.87. Therefore, the DMPC achieves nearly the centralized MPC closed-loop performance.

Finally, we compare centralized MPC and DMPC from a control action evaluation time point of view. We set the horizon of MPC to $N=30$. We compute the average evaluation time of the MPC formulation at mode 1 (40 times) which includes the switching constraint and the MPC after we switch to mode 2 (960 times) in both centralized and DMPC formulations. For the DMPC design, we add the simulation time of two iterations and since the three controllers optimize in parallel, we consider the maximum time of the computational time of the distributed controllers as the computational time of the DMPC. The result indicates that for mode 1 there is an almost 36% improvement ($\max\{10418, 38.27, 16429\}$ s vs. 259.50 s) and for mode 2 there is an almost 39% improvement ($\max\{3170, 32.99, 3768\}$ s vs. 63.41 s) in computational time when we use the DMPC framework compared to the centralized MPC while the closed-loop performance remains nearly the same.

Conclusions

This work focused on the design of DMPC systems for a class of switched nonlinear systems subject to a prescribed switching policy. Under appropriate stabilizability assumptions, the proposed DMPC systems ensure closed-loop stability and satisfaction of the switching policy. Convergence of the DMPC optimal solution to the corresponding centralized MPC optimum was established for the linear case. A chemical process network example was used to demonstrate the proposed DMPC design method.

Literature Cited

1. Branicky MS. Multiple Lyapunov functions and other analysis tools for switched and hybrid systems. *IEEE Trans Automat Control*. 1998;43:475–482.
2. Hespanha JP, Morse AS. Stability of switched systems with average dwell-time. In *Proceedings of the 38th IEEE Conference on Decision and Control*, Phoenix, Arizona, 1999:2655–2660.
3. Liberzon D. *Switching in Systems and Control*. Boston, MA: Springer, 2003.
4. Lin H, Antsaklis PJ. Stability and stabilizability of switched linear systems: a survey of recent results. *IEEE Trans Automat Control*. 2009;54:308–322.
5. Daafouz J, Riedinger P, Iung C. Stability analysis and control synthesis for switched systems: a switched Lyapunov function approach. *IEEE Trans Automat Control*. 2002;47:1883–1887.
6. El-Farra NH, Christofides PD. Coordinating feedback and switching for control of hybrid nonlinear processes. *AIChE J*. 2003;49:2079–2098.
7. Han TT, Ge SS, Lee TH. Adaptive neural control for a class of switched nonlinear systems. *Syst Control Lett*. 2009;58:109–118.
8. Hespanha JP, Morse AS. Switching between stabilizing controllers. *Automatica*. 2002;38:1905–1917.
9. Yang H, Cocquempot V, Jiang B. On stabilization of switched nonlinear systems with unstable modes. *Syst Control Lett*. 2009;58:703–708.
10. Borrelli F, Baotic M, Bemporad A, Morari M. Dynamic programming for constrained optimal control of discrete-time linear hybrid systems. *Automatica*. 2005;41:1709–1721.
11. Gorges D, Izak M, Liu S. Optimal control and scheduling of switched systems. *IEEE Trans Automatic Control*. 2011;56:135–140.
12. Mayne DQ, Rawlings JB, Rao CV, Scokaert POM. Constrained model predictive control: stability and optimality. *Automatica*. 2000;36:789–814.
13. Cassandras C, Mookherjee R. Receding horizon optimal control for some stochastic hybrid systems. In *Proceedings of 41th IEEE Conference on Decision and Control*, Maui, Hawaii, 2003:2162–2167.
14. Mhaskar P, El-Farra NH, Christofides PD. Predictive control of switched nonlinear systems with scheduled mode transitions. *IEEE Trans Automat Control*. 2005;50:1670–1680.
15. Lazar M, Heemels W, Weiland S, Bemporad A. Stabilizing model predictive control of hybrid systems. *IEEE Trans Automat Control*. 2006;51:1813–1818.
16. Lazar M, Heemels W. Predictive control of hybrid systems: Input-to-state stability results for sub-optimal solutions. *Automatica*. 2009;45:180–185.
17. Camponogara E, Jia D, Krogh BH, Talukdar S. Distributed model predictive control. *IEEE Control Syst Mag*. 2002;22:44–52.
18. Rawlings JB, Stewart BT. Coordinating multiple optimization-based controllers: new opportunities and challenges. *J. Process Control*. 2008;18:839–845.
19. Scattolini R. Architectures for distributed and hierarchical model predictive control—a review. *J Process Control*. 2009;19:723–731.
20. Christofides PD, Liu J, Muñoz de la Peña D. *Networked and Distributed Predictive Control: Methods and Nonlinear Process Network Applications*. Advances in Industrial Control Series. London, England: Springer-Verlag, 2011.
21. Christofides PD, El-Farra NH. *Control of Nonlinear and Hybrid Process Systems: Designs for Uncertainty, Constraints and Time-Delays*. Berlin, Germany: Springer-Verlag, 2005.
22. Lin Y, Sontag ED, Wang Y. A smooth converse Lyapunov theorem for robust stability. *SIAM J Control Optim*. 1996;34:124–160.
23. Bertsekas DP, Tsitsiklis JN. *Parallel and Distributed Computation*. Belmont, MA: Athena Scinetific, 1997.
24. Stewart BT, Venkat AN, Rawlings JB, Wright SJ, Pannocchia G. Cooperative distributed model predictive control. *Syst Control Lett*. 2010;59:460–469.
25. Christofides PD, Scattolini R, Muñoz de la Peña D, Liu J. Distributed model predictive control: a tutorial review and future research directions. *Comput Chem Eng*. DOI: 10.1016/j.compchemeng.2012.05.011
26. Chilin D, Liu J, Muñoz de la Peña D, Christofides PD, Davis JF. Detection, isolation and handling of actuator faults in distributed model predictive control systems. *J Process Control*. 2010;20:1059–1075.
27. Lin Y, Sontag ED. A universal formula for stabilization with bounded controls. *Syst Control Lett*. 1991;16:393–397.

Manuscript received Oct. 11, 2012, and revision received Dec. 9, 2012.